NUMERICAL SIMULATIONS OF CHICXULUB CRATER FORMATION BY OBLIQUE IMPACT.
G. S. Collins[1], N. Patel[1], A. S. P. Rae[1], T. M. Davison[1], J. V. Morgan[1], S. Gulick[2] and Expedition 364 Scientists,
[1]Department of Earth Science and Engineering, Imperial College London, SW7 2BP, UK, g.collins@imperial.ac.uk.
[2]Department of Geological Sciences, University of Texas at Austin, TX 78758, USA.

Introduction: Impact trajectory direction and angle to the target plane are important impact parameters that determine the direction of most severe environmental consequences and the volume and depth of origin of vaporized target [1], as well as ejecta [2] and crater asymmetries [3]. Asymmetries in the subsurface structure of the Chicxulub crater have been linked to asymmetry in the preimpact target [4, 5], as well as impact angle and direction [1, 6], but those parameters are debated. Here we use 3D numerical modeling to examine the relationship between impact angle and structural crater asymmetries in a Chicxulub-scale peak-ring crater without preimpact target asymmetry.

Methods: The Chicxulub impact was simulated using the iSALE3D shock physics code [7, 8], with equations of state [9, 10] and a strength model [11] appropriate for crustal and mantle rocks. The choice of model parameters was based on previous vertical impact simulations using iSALE2D [12, 5, 13] and oblique impact simulations of the early stages of the Chicxulub impact [14]. A mean crustal thickness of 33 km was used. Material number limitations precluded inclusion of a rheologically distinct sedimentary layer in the target; however, tracer particles allowed material at this stratigraphic level to be tracked during the simulation, as well as the peak shock pressure and provenance of peak ring materials. We considered four impact angles: 90° (vertical), 60°, 45° and 30°. A low impact speed (12 km/s) was used for computational expediency and to afford direct comparison of the vertical impact case with previous 2D simulations. Impactor diameter was increased with decreasing impact angle (from 16 km at 90° to 21 km at 30°) to achieve approximately equivalent final crater diameters (<12% difference). Common acoustic fluidization parameters (viscosity and decay time) were used in all simulations. The minimum cell size was 500 m, affording resolutions of 16-21 cells per impactor radius, depending on impact angle.

Results & Discussion: Oblique impact simulations of Chicxulub crater formation produce along-range asymmetries in crater evolution, final peak-ring and crater structure and surface morphology that in general become increasingly pronounced with decreasing impact angle to the target surface (Figs. 1 & 2).

Compared with the vertical impact case, oblique impact results in less uplift of the transient crater rim in the uprange direction and more uplift in the downrange direction. Subsequent rebound of the crater floor during crater collapse begins uprange of the crater centre, but has a downrange component such that the central uplift is tilted downrange and the centre of the uplift prior to its collapse is downrange of the crater centre (Fig. 2). Conversely, downward and outward collapse of the central uplift occurs preferentially in the uprange direction, resulting in enhanced overthrusting of the central uplift on top of transient crater rim in the uprange direction. The net result of the downrange-directed rise and uprange-directed fall of the central uplift is a peak ring with a centre only modestly offset in the downrange direction (Fig. 1).

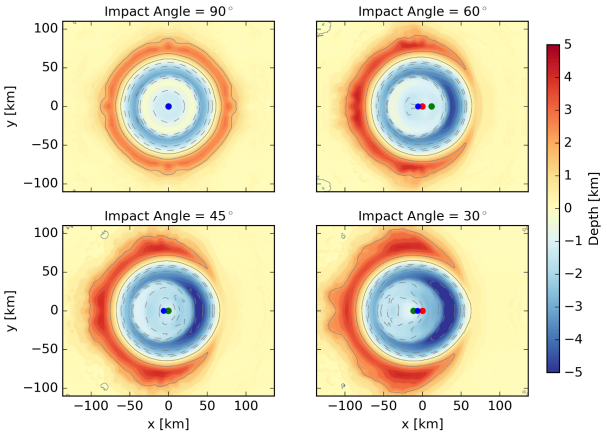

Figure 1: Surface topography of simulated Chicxulub crater, for different impact angles (to the target plane), immediately after peak-ring formation (T = 5 mins). Impact direction is right to left. Green dot indicates centre of mantle uplift; red dot - centre of crater; blue dot - centre of peak ring.

Asymmetry in crater development produces differences in final crater structure in the uprange and downrange directions. Interestingly, while the centre of the peak ring appears to be consistently offset downrange of the crater centre by ~5% of the crater diameter in the three oblique impacts, the centre of the mantle uplift is offset uprange of the crater centre in the 60° impact; is coincident with the crater centre at 45°; and is offset downrange in the 30° impact (Fig. 1). Geophysical observations at Chicxulub suggest the peak-ring and mantle-uplift centres are offset in different directions from the crater centre, in a configuration similar to the 60° impact simulation.

Tracer particles that track the history of material in the simulation afford analysis of the provenance and shock state of peak ring materials and their variation with azimuth. Approximately 80% of unmelted peak ring material experiences a shock pressure of 20-40

GPa with only a weak dependence on impact angle above 30°. Similarly, the fraction of impact melt in the peak ring materials is consistently 10-15% for all impact angles. Asymmetry in shock wave strength results in slightly reduced shock pressures and a lower fraction of impact melt in the uprange direction. In the 30° impact, melt fraction drops to zero and mean shock pressure by a factor of two in the uprange quadrant.

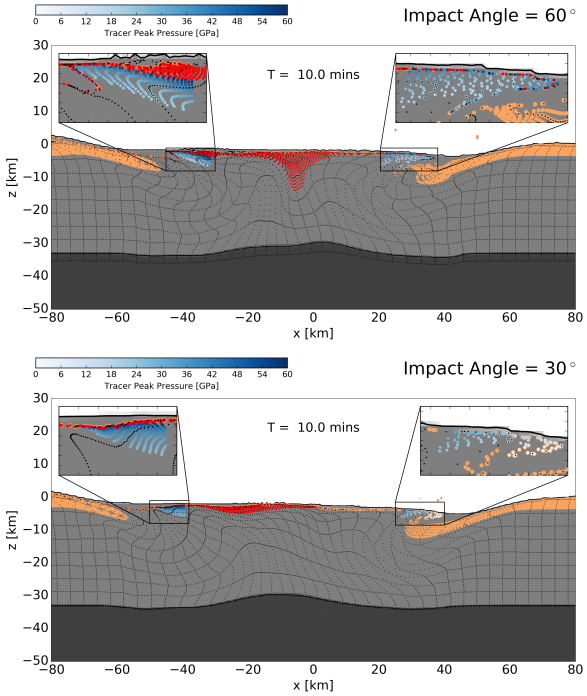

Figure 2: Cross-sections of the final simulated Chicxulub crater, in the plane of the impact trajectory, for a 60° (top) and 30° (bottom) impact angle (to the target plane). Impact direction is right to left. Green tracers indicate the final position of the upper 3-km of the preimpact target (sediments); red tracers indicate the position of melt; tracers with blue-white shading indicate shock pressures of peak-ring materials. The geometric centre of the crater rim defines the coordinate origin ($x = 0$); negative x-values are downrange.

The mean depth of origin of peak ring materials is 10-12 km for the 45°, 60° and 90° impacts, only dropping significantly, to ~8 km, in the 30° impact. In this case azimuthal variation is negligible apart from the uprange quadrant, within which the peak ring materials are sourced from shallower depths. In the 30° scenario a significant fraction of the peak ring originates from the sedimentary sequence in the uprange direction (Fig. 2), which is not consistent with geophysical interpretations or results from Expedition 364 [13].

We also observe a systematic change in the up-/downrange difference in subsurface structure of peak rings with impact angle (Fig. 2). Similar to the situation in a vertical impact, at 60° the peak ring is formed of overthrusted granitic crustal rocks from the central uplift above down-slumped sediments from the transient crater wall, in all directions. However, the sediments are deeper and extend farther beneath the peak ring in the uprange direction, compared to the downrange direction (Fig. 2). At 45° and 30° this difference is more pronounced, to the point that in the downrange direction, because of enhanced transient crater rim uplift on this side of the crater, the inwardly slumped sediments do not extend under the peak ring (Fig. 2). This downrange configuration is inconsistent with geophysical interpretations at Chicxulub, which suggest sedimentary slump blocks lie beneath the outer portion of the peak ring at all azimuths offshore. However, preimpact asymmetries in sediment thickness, water depth, particularly in the NE part of the crater (and potentially in the crust), may also affect structure beneath the peak ring.

Conclusions: Comparison of our numerical simulation results with geophysical interpretations at Chicxulub suggest that the Chicxulub crater was formed by a steep angle (>45) impact. Several lines of evidence rule out a low-angle impact. This is consistent with symmetric distribution of ejecta [15, 14, 16]. Azimuthal variation in peak-ring material properties (shock pressure, depth of origin, etc.) is small, suggesting that the results of IODP Expedition 364 are likely to be representative of the general character of the Chicxulub peak ring.

Acknowledgments: We gratefully acknowledge the developers of iSALE (www.isale-code.de), in particular, Dirk Elbeshausen. This work was funded by STFC (ST/J001260/1) and NERC (NE/P011195/1).

References: [1] Schultz PH & D'Hondt S (1996) *Geology* 24: 963–967. [2] Gault DE & Wedekind J (1978) *Proc. LPSC,* 9: 3843–3875. [3] Scherler D, et al. (2006) *EPSL* 248: 43–53. [4] Gulick S, et al. (2008) *Nature Geoscience* 1: 131–135. [6] Hildebrand AR, et al. (1998) *LPSC XXIX*, Houston, TX. Abs. #1821. [7] Elbeshausen D, et al. (2009) *Icarus*, 204:716–731. [8] Amsden AA & Ruppel HM (1981) LANL Report LA-8905. Los Alamos, New Mexico, 151 p. [9] Pierazzo E, et al. (1997) *Icarus*: 127(2): 408–423. [10] Benz W, et al. (1989) *Icarus*, 81(1): 113–131. [11] Collins GS, et al. (2004) *M&PS*, 39: 217–231. [12] Ivanov BA (2005) *SSR*, 39:381– 409. [5] Collins GS, et al. (2008) *EPSL*, 270: 221–230. [13] Morgan JV, et al. (2016) *Science*, 354(6314): 878-882. [14] Artemieva N & Morgan J (2009) *Icarus* 201: 768–780. [15] Morgan JV, et al. (2006) *EPSL*, 251: 264-279. [16] Bermúdez HD, et al. (2016) *Terra Nova*, 28: 83-90.